ESC HEART FAILURE
ESC Heart Failure 2022; **9**: 303–317
Published online 28 December 2021 in Wiley Online Library (wileyonlinelibrary.com) **DOI:** 10.1002/ehf2.13754

ORIGINAL ARTICLE

Exacerbated post-infarct pathological myocardial remodelling in diabetes is associated with impaired autophagy and aggravated NLRP3 inflammasome activation

Shuai Mao[1,2,3], Peipei Chen[1,2], Wenjun Pan[1,2], Lei Gao[4] and Minzhou Zhang[1,2,3]*

[1]*Second Clinical College, Guangzhou University of Chinese Medicine, Guangzhou, China;* [2]*Department of Critical Care Medicine, Guangdong Provincial Hospital of Chinese Medicine, Guangzhou, 510120, China;* [3]*Guangdong Provincial Branch of National Clinical Research Centre for Chinese Medicine Cardiology, Guangzhou, China; and* [4]*Department of Medicine, University of California San Diego, La Jolla, CA, USA*

Abstract

Background Diabetes mellitus (DM) patients surviving myocardial infarction (MI) have substantially higher mortality due to the more frequent development of subsequent pathological myocardial remodelling and concomitant functional deterioration. This study investigates the molecular pathways underlying accelerated cardiac remodelling in a well-established mouse model of diabetes exposed to MI.

Methods and results Myocardial infarction in DM mice was established by ligating the left anterior descending coronary artery. Cardiac function was assessed by echocardiography. Myocardial hypertrophy and cardiac fibrosis were determined histologically 6 weeks post-MI or sham operation. Autophagy, the NLRP3 inflammasome, and caspase-1 were evaluated by western blotting or immunofluorescence. Echocardiographic imaging revealed significantly increased left ventricular dilation in parallel with increased mortality after MI in DM mice (53.33%) compared with control mice (26.67%, $P < 0.05$). Immunoblotting, electron microscopy, and immunofluorescence staining for LC3 and p62 indicated impaired autophagy in DM + MI mice compared with control mice ($P < 0.05$). Furthermore, defective autophagy was associated with increased NLRP3 inflammasome and caspase-1 hyperactivation in DM + MI mouse cardiomyocytes ($P < 0.05$). Consistent with NLRP3 inflammasome and caspase-I hyperactivation, cardiomyocyte death and IL-1β and IL-18 secretion were increased in DM + MI mice ($P < 0.05$). Importantly, the autophagy inducer and the NLRP3 inhibitor attenuated the cardiac remodelling of DM mice after MI.

Conclusion In summary, our results indicate that DM aggravates cardiac remodelling after MI through defective autophagy and associated exaggerated NLRP3 inflammasome activation, proinflammatory cytokine secretion, suggesting that restoring autophagy and inhibiting NLRP3 inflammasome activation may serve as novel targets for the prevention and treatment of post-infarct remodelling in DM.

Keywords Pathological myocardial remodelling; Diabetes mellitus; Autophagy; NLRP3 inflammasome

Received: 31 March 2021; Revised: 28 October 2021; Accepted: 24 November 2021
**Correspondence to: Minzhou Zhang, Department of Critical Care Medicine, Guangdong Provincial Hospital of Chinese Medicine, Guangzhou 510120, China. Phone: +86-20-81887233; Fax: +86-20-81867705. Email: minzhouzhang@gzucm.edu.cn*

Introduction

Despite recent progress in coronary intervention strategies, patients with diabetes mellitus (DM) continue to experience a higher risk of adverse cardiovascular events after myocardial infarction (MI), including the development of heart failure and even cardiogenic death, than patients without DM worldwide.[1] In particular, recurrent MI rates are 1.7 to 4 times higher after MI in diabetic patients than in non-diabetic subjects, with a 12 month mortality rate in this

population as high as 50%.[2,3] The poor prognosis of diabetic patients after MI has been explained by underlying left ventricle (LV) remodelling.[4] MI leads to exaggerated cardiomyocyte death and initiates inflammatory responses, contributing to heart failure.[5] At the organ level, the LV undergoes a complex remodelling procedure to compensate for the reduced cardiac function after MI. Failure to compensate will eventually lead to infarct expansion, global ventricular dilation, myocardial hypertrophy, cardiac fibrosis, and finally, heart failure.[6] The cellular and molecular pathways contributing to maladaptive ventricle remodelling and heart failure after MI in diabetic patients are poorly understood, and uncovering the underlying pathophysiological mechanisms may lead to targeted therapies for diabetic patients with MI.

One of the most recently identified proinflammatory signalling pathways in post-infarct adverse remodelling is the NOD-like receptor pyrin domain-containing-3 (NLRP3) inflammasome. It has been demonstrated that activated NLRP3 inflammasomes promote the maturation and secretion of proinflammatory cytokines, especially the interleukin (IL)-1 family and IL-18, which are considered potent inducers contributing to myocardial remodelling.[7] Moreover, these cytokines of the IL-1 family modulate the insulin-producing pancreatic ?-cell function and act as inflammatory mediators in pathological remodelling.[8] Distinct from pyroptosis, apoptosis, and necrosis, autophagy protects against the development of cardiac hypertrophy and failure.[9] Loss of cardiac Atg5-dependent autophagy impairs cardiac contractile capacity in mice and humans by diminishing mitochondrial abundance and disrupting Ca^{2+} cycling.[10] This is in line with animal models of type 2 diabetes mellitus (T2DM), inhibition of mTOR either by AAV-mediated overexpression of PRAS40, or rapamycin increased autophagy, which correlated with reduced hypertrophy and improved cardiac function.[11,12] In contrast, inhibition of autophagy with 3-methyladenine (3MA) exacerbated pressure overload-induced cardiac hypertrophy and dysfunction.[13] However, whether autophagy is cardioprotective or deleterious in post-MI pathological remodelling in the context of DM remains to be elucidated.

Herein, we have addressed the molecular pathways underlying left ventricular pathological remodelling after MI in a well-established mouse model of DM.[14] These mice demonstrate typical features of human DM, including hyperglycaemia and mild hyperinsulinemia. In addition, these diabetic mice show exacerbated post-infarct pathological myocardial remodelling. With the use of molecular characterization, we found a damaged autophagy and NLRP3 inflammasome overactivation in cardiomyocytes from the peri-infarct zone of the LV in diabetic mice. Moreover, deteriorated autophagy and aggravated NLRP3 inflammasome activation were associated with increased cardiomyocyte death and proinflammatory cytokine secretion (IL-1β and IL-18), which contributed to maladaptive LV remodelling after MI. Modulation of autophagy together with inhibition of inflammasome activation may offer a novel therapeutic approach for the prevention of post-infarct pathological remodelling in DM.

Methods

Experimental design

The experimental procedures were approved by the Institutional Animal Care and Use Committee of Guangdong Province Hospital of Chinese Medicine at Guangzhou University of Chinese Medicine and performed in accordance with Guide for the Care and Use of Laboratory Animals published by the US National Institutes of Health (publication No. 85–23, revised 1996).

Male C57BL/6J mice, aged 5–6 weeks, used in this study were purchased from Experimental Animal Center of Guangdong Province (Guangzhou, China). Mice model of T2DM were induced by once daily Streptozotocin (STZ) 50 mg/kg by intraperitoneal injection (three continuous days).[15] To induce insulin resistance, DM mice were fed with a high-fat diet (D12492, Research Diets, New Brunswick, NJ, USA) during the study.[16] After 3 days of STZ administration, MI was induced surgically by chronic ligation of the left anterior descending coronary artery, as described previously.[6] Mice in control group underwent sham-operated surgery, but the left anterior descending coronary artery was not ligated.

According to the indicated administration and surgery, mice were allocated to one of six groups (Supporting Information, *Table* S1): mice received sham operation (control, n = 15), mice received MI operation (MI, n = 15), DM mice received sham operation (DM, n = 15), DM mice received MI operation (DM + MI, n = 15), DM + MI mice given rapamycin (autophagy inducer, n = 15), DM + MI mice given 3MA (mTOR/autophagy inhibitor, n = 15), and DM + MI mice given MCC950 (NLRP3 inflammasome inhibitor, n = 15). Rapamycin was intraperitoneally injected at the dose of 5 mg/kg twice per week for 6 weeks. The 3MA was administered by intraperitoneal injection (15 mg/kg, twice per week) for 6 weeks. MCC950 was intraperitoneally injected at the dose of 5 mg/kg twice per week for 6 weeks. These doses of 3MA, rapamycin, and MCC950 were previously reported not to cause apparent adverse effects in the rodent heart.[17,18] All reagents were obtained from Sigma-Aldrich Chemicals (St. Louis, MO, United States) unless otherwise specified. Body weight, food and water consumption, fasting glucose, and glycated haemoglobin were assessed. Survival rate was assessed until 6 weeks after surgery. On Day 45 after surgery, mice were euthanized with pentobarbital for subsequent echocardiographic and LV histologic analyses.

Transthoracic echocardiography

Left ventricle function and structure of mice were examined with echocardiography under 1% isoflurane anaesthesia via the Vevo 770 high-resolution imaging system (Visual Sonics, Toronto, Canada) in a blinded fashion by the same technician before and 3 days and 6 weeks after coronary ligation as described previously.[19] The two-dimensional imaging (Teichholz method) targeted echocardiographic recordings were acquired at the level of the papillary muscles. LV end-diastolic dimension and LV end-systolic dimension were averaged from more than five cardiac cycles.

Pathological examination

After perfusion with phosphate-buffered saline, hearts were embedded in paraffin and cut as 5-μm-thick section. Infarct scar circumference and myocardial fibrosis were studied via Masson's trichrome stains. Cardiomyocyte cross-sectional area was quantitatively determined on haematoxylin and eosin stained slides with computer-assisted methods described previously.[5]

Immunofluorescence microscopy

To observe autophagic activity in the cardiomyocytes, sections immunostained with primary antibodies at 10 μg/mL were anti-LC3 (MBL International, Woburn, MA, US), anti-NLRP3 (Thermo Fisher Scientific, Pleasanton, CA, US), anti-Caspase-1 (Thermo Fisher Scientific, Pleasanton, CA, US), and followed by Alexa 568 (red, Molecular Probes, Sunnyvale, CA, US). Nuclei were stained with 4′-6-diamidino-2-phenylindole. All immunostained sections were assessed under a Nikon Eclipse E1000 microscope and Nikon Digital Sight Camera (Nikon Instruments, Tokyo, Japan).

Terminal deoxynucleotidyl transferase dUTP nick end labelling assay

The DNA fragmentations from nuclei of cardiomyocytes in LV tissue sections were determined using a Fluorescein-FragEL kit (Oncogene Research Products, Boston, MA, United States). TUNEL-positive cells were counted and analysed in more than 10 high power fields using NIS-Element imaging software (Nikon Instruments, Tokyo, Japan).

Electron microscopy

Left ventricle tissue sections were quickly cut into 1 mm^3 and fixed with glutaraldehyde in sodium cacodylate buffer overnight at 4°C. Ultrathin sections of approximately 70 nm were double stained with lead citrate and uranyl acetate and imaged with transmission electron microscopy (Olympus Soft Imaging Solutions GmbH, Münster, Germany). Autophagosomes or autolysosomes were identified by the characteristic structure of a double or multilamellar smooth membrane completely surrounding compressed mitochondria or membrane-bound electron-dense material. For quantification, 15 random regions for each sample were considered.

Enzyme-linked immunosorbent assay

Levels of inflammatory cytokines including tumour necrosis factor (TNF)-α, IL-1β, IL-6, IL-18, and high mobility group box 1 (HMGB-1) in the LV tissue were measured using commercially available ELISA kits (BioTech, MN, United States). All spectrophotometric readings were obtained with a microplate reader according to the manufacturer's instructions (Multiskan MK3, Thermo Scientific, United States).

Quantitative real-time RT-PCR analysis

Total RNA from LV tissue was prepared using the RNAspin Mini Kit (GE Healthcare, Marlborough, MA, USA). Reverse transcription of RNA was performed using SuperScriptTM II Reverse Transcriptase with random primers (Invitrogen, USA) following the manufacturer's protocol. PCR reaction was carried out in a total reaction volume of 15 μL, including: 7.5 μL of SYBR® Green PCR master mix (Applied Biosystems, CA), 5 ng of cDNA template, and 0.2 μM of gene-specific primers. Real-time PCR was carried out using an ABI Prism 7900HT (Applied Biosystems, Foster City, CA). Changes in mRNA expression in NLRP3, Caspase-1, LC3a, and P62 was normalized to 18 s mRNA levels and compared statically ($^{\Delta\Delta}$Ct method) using the ABI Prism SDS 2.1 software.

Western blot analysis

Left ventricle samples were solubilized using ice-cold Nonidet P-40 lysis buffer. The prepared samples were analysed using western blotting as previously described.[20] Briefly, after boiled in sample buffer for 5 min, 30 μg of the protein extract was separated with 8–15% sodium dodecyl sulfate-polyacrylamide gel, and then transferred onto a polyvinylidene difluoride membrane. The membrane was probed first with primary antibodies (anti-GAPDH, anti-NLPR3, anti-cleaved caspase1, anti-p62, and anti-LC3) overnight at 4°C and subsequently incubated with a horseradish peroxidase-conjugated secondary antibody for 2 h at room temperature following by incubation with enhanced chemiluminescent substrate (Amersham Life Sciences Inc., Marlborough, MA, US). Protein expression or phosphorylation of immunodetected signalling molecules was quantified

by densitometry (Chemidoc, Biorad, US). All experiments were separately repeated at least three times.

Statistical analysis

Data are presented as means ± SE. Statistical significance was evaluated with one-way analysis of variance or by Student's *t*-test using SPSS software Version 13.0 (SPSS, Inc., Armonk, NY, US). The cumulative survival rate of the mice after MI was analysed by the Kaplan–Meier method with a log-rank test. Values of $P < 0.05$ were considered statistically significant.

Results

Diabetes mellitus accelerates mortality and deteriorates left ventricular dilation and dysfunction after myocardial infarction

During the first 3 days after coronary ligation, mice with or without DM had similar mortality rates (6.67%, $P > 0.05$). However, 53.33% of DM + MI mice died during the 42 days after coronary ligation, whereas only 26.67% of mice without DM died during the same period. The overall survival rates of the DM + MI group were considerably lower than those of the MI group (46.67% vs. 73.33%, $P < 0.05$). No mice with or without DM died after the sham operation (*Figure 1A*).

Echocardiographic assessment was performed to evaluate the cardiac function of mice at baseline and 6 weeks after coronary ligation. At baseline, mice showed non-significant differences in left ventricular structure and function in all groups. Representative M-mode images and quantitative analysis of cardiac parameters at 6 weeks after MI are shown in *Figure 1B* and *Table S2*. In response to MI, a marked increase in left ventricular chamber dilation and systolic dysfunction was observed in both the DM + MI and MI groups compared with their respective sham controls. Moreover, compared with the MI group, the DM + MI group demonstrated a significant increase in LV end-diastolic dimension and LV end-systolic dimension at 6 weeks after coronary ligation (*Figure 1B* & *Table S2*). Additionally, significant systolic dysfunction was exacerbated, as assessed by left ventricular ejection fraction (LVEF) and left ventricular fractional shortening, in DM + MI mice compared with the MI group ($P < 0.05$). Along with left ventricular dilation, haemodynamic analysis suggested a lower stroke volume in the DM + MI group than in the MI group (*Figure 1B* & *Table S2*). Collectively, these data indicated that DM adversely influenced cardiac dilation and function and increased the mortality rate in response to MI.

Diabetes mellitus aggravates ventricular remodelling and fibrosis after myocardial infarction

Diabetes mellitus mice displayed an increased body weight and blood glucose levels at baseline. However, the heart weight to body weight ratio was comparable between the groups at baseline. After MI, the heart undergoes structural remodelling, resulting in a more spherical shape. Isolated hearts from the DM + MI group demonstrated an increase in heart weight/body weight compared with those from the MI group 6 weeks after MI, indicating that DM exaggerated global cardiac remodelling in mice with MI (*Figure 2A*).

In DM + MI mice, the post-infarction scar comprised a much larger percent circumference of LV than in the MI group (23.4 ± 4.31% vs. 42.2 ± 6.42%, $P < 0.05$), indicating that the infarct scar expansion was intensified by DM (*Figure 2B*).

Interstitial fibrosis, a hallmark of cardiac remodelling, was increased in the DM + MI heart compared with the MI group (19.23 ± 4.10% vs. 45.66 ± 7.62%, $P < 0.05$, *Figure 2C*).

Myocyte size was analysed in the border and the remote zones (*Figure 2D*). Decreased myofilament density and increased myocyte size were observed in the border zone of the DM + MI group compared with the MI group. In contrast, no significant difference in either myofilament density or myocyte size was observed in the remote zone between the two groups, suggesting that DM exacerbated myocyte hypertrophy and secondary cell loss in the border zone after MI. In concert, these results reveal that DM exaggerates ventricular remodelling and fibrosis after MI.

Diabetes mellitus increased inflammatory cytokine expression in mice subjected to myocardial infarction

Myocardial ischaemia initiates an inflammatory response characterized by an accumulation of leukocytes in the injured myocardium, while cytokine expression further promotes adverse LV remodelling.[21] To elucidate the effect of DM on post-infarct inflammation, the expression of TNF-α, IL-1β, IL-6, HMGB-1, and IL-18 in the myocardium was evaluated using commercial ELISA kits. The results showed that the expressions of these inflammatory factors in the DM + MI myocardium tissue dramatically increased compared with that in the MI group (*Figure 3A*).

In parallel, there was a remarkable increase in immune-detectable antibodies against the inflammatory factors TNF-α, IL-1β, IL-6, HMGB-1, and IL-18 in the presence of DM in the myocardium after MI, which further supports the ELISA results (*Figure 3B*). Of note, increased inflammation as evidenced by increased IL-1β, IL-18, and

Figure 1 DM increased mortality and deteriorated cardiac dysfunction after MI. (A) Kaplan–Meier survival curves after MI for control and DM mice 42 days after MI. (B) Representative M-mode images and quantitative analysis of cardiac parameters, including LVEDV, LVESV, LVEF, LVFS, and SV at 42 days after MI. Data are expressed as means ± SEM. $^{\#}P < 0.05$ DM + MI vs. MI; $^{*}P < 0.05$ MI vs. controls. DM, diabetes mellitus; LVEDV, left ventricular end-diastolic volume; LVEF, left ventricular ejection fraction; LVESV, left ventricular end-systolic volume; LVFS, left ventricular fractional shortening; MI, myocardial infarction; SV, systolic volume.

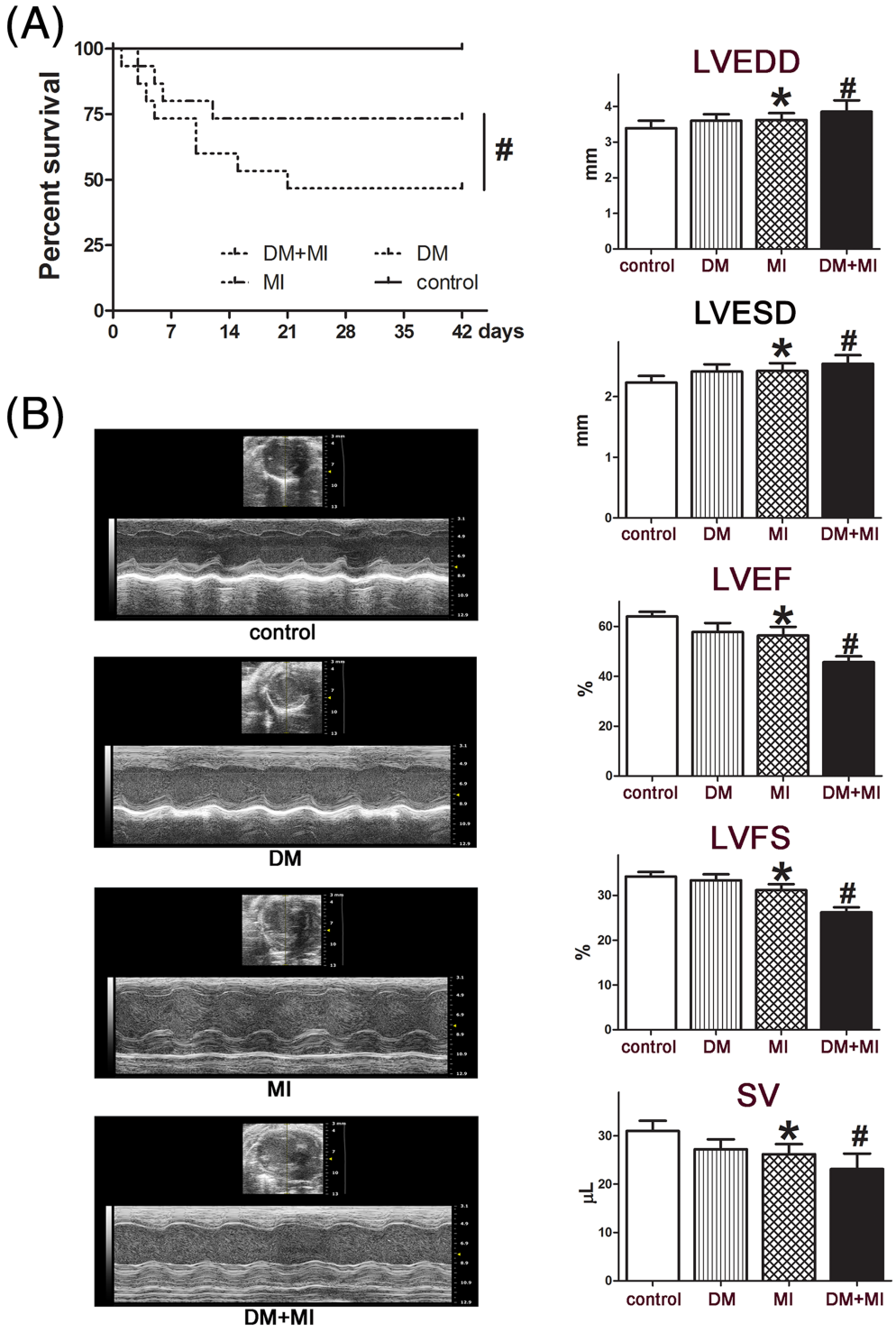

DOI: 10.1002/ehf2.13754

Figure 2 DM exacerbated cardiac remodelling and myocardial injury after MI. (A) Hearts from DM + MI mice appear more spherical than those from MI and DM mice (scale bar = 3 mm). (B, C) Paraffin-embedded sections of myocardium were stained with Masson's trichrome showing the effects of DM on scar circumference (scale bar = 5 mm) and ventricular fibrosis (scale bar = 50 μm). (D) Representative image of haematoxylin and eosin showing cardiomyocyte size from mice (scale bar = 50 μm). $^{\#}P < 0.05$ DM + MI vs. MI; $^{*}P < 0.05$ MI vs. controls. BW, body weight; DM, diabetes mellitus; HW, heart weight; MI, myocardial infarction.

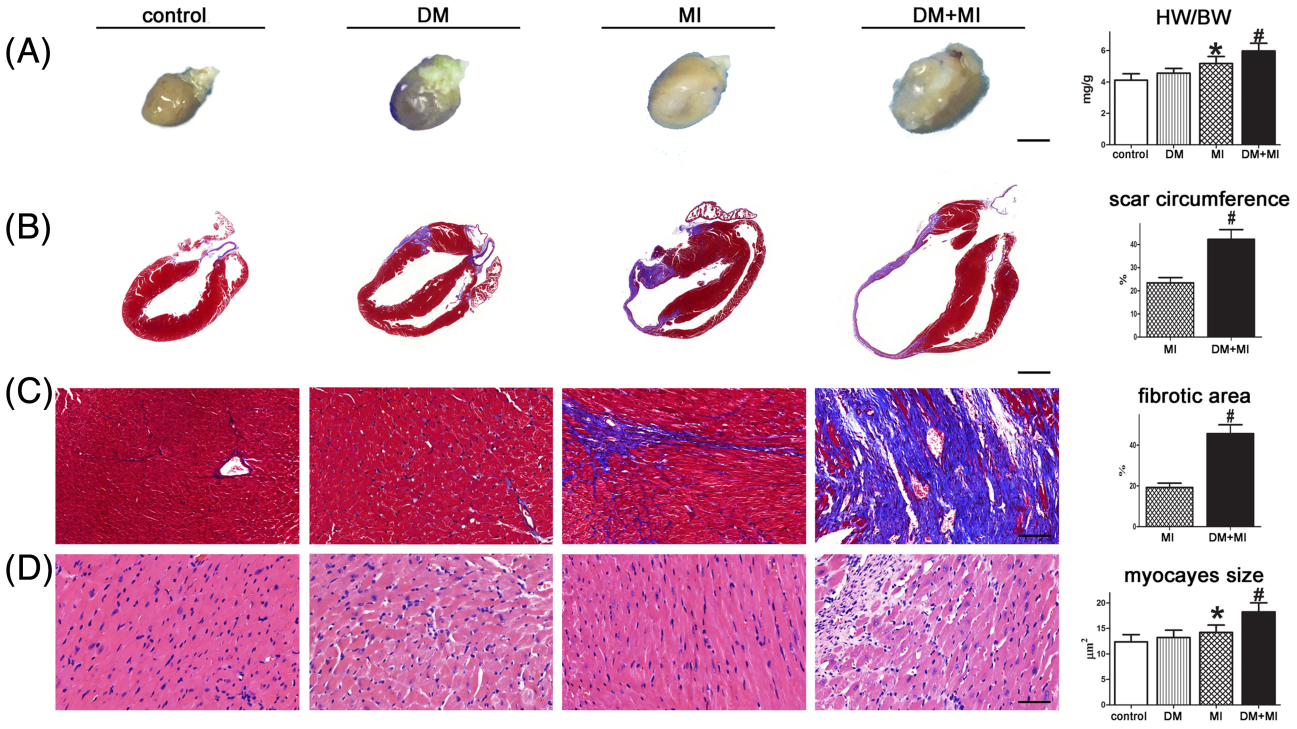

circulating immune cells was shown to be associated with remodelling and HF after MI in patients.

Diabetes mellitus exaggerated NLRP3 inflammasome and caspase-1 activation in mice after myocardial infarction

Cardiomyocyte pyroptosis and apoptosis contribute to post-infarct cardiac remodelling and subsequent cardiac dysfunction.[22] Both the mRNA and protein levels of the NLRP3 inflammasome were significantly up-regulated in peri-infarct regions of the LV in DM + MI mice compared with the MI group (*Figure 4A*, *B*). Furthermore, immunofluorescence staining for NLRP3 showed increased activation from peri-infarct regions of LV in DM + MI compared with the MI group (*Figure 4C*).

NLRP3 inflammasome activation triggers in caspase-1-mediated classical pyroptosis and subsequent cytokine processing into mature active forms (IL-1β and IL-18).[23] To understand the consequence of NLRP3 inflammasome activation, caspase-1 activity was examined by RT-PCR, immunoblotting and immunostaining of LV tissue after MI. Similar to NLRP3, the results demonstrated increased activation of caspase-1 in peri-infarct regions of the LV in both the DM + MI and MI groups (*Figure 4A*, *B*, and *C*). Furthermore, caspase-1 showed increased activity in DM + MI mice compared with MI mice (*Figure 4A*, *B*, and *C*).

Next, cell death was examined with the TUNEL assay, and a dramatically increased number of TUNEL-positive cells were observed on the border of the MI hearts from DM + MI mice compared with the MI mice (*Figure 4D*). Collectively, these results indicated that DM exaggerated activation of the NLRP3 inflammasome and a subsequent increase in caspase-1-mediated cell death (pyroptosis) and inflammatory factor (IL-1β and IL-18) maturation in peri-infarct regions of the LV.

Diabetes mellitus impaired autophagy in cardiomyocytes of the peri-infarct region

Increasing evidence has shown that autophagy is involved in the regulation of LV remodelling; therefore, we investigated cardiomyocyte autophagy in the present study.[24] The qRT-PCR results showed that the level of LC3a was significantly down-regulated, while the level of SQSTM1/p62 was up-regulated in the peri-infarct regions of the LV from DM + MI mice compared with MI mice (*Figure 5A*).

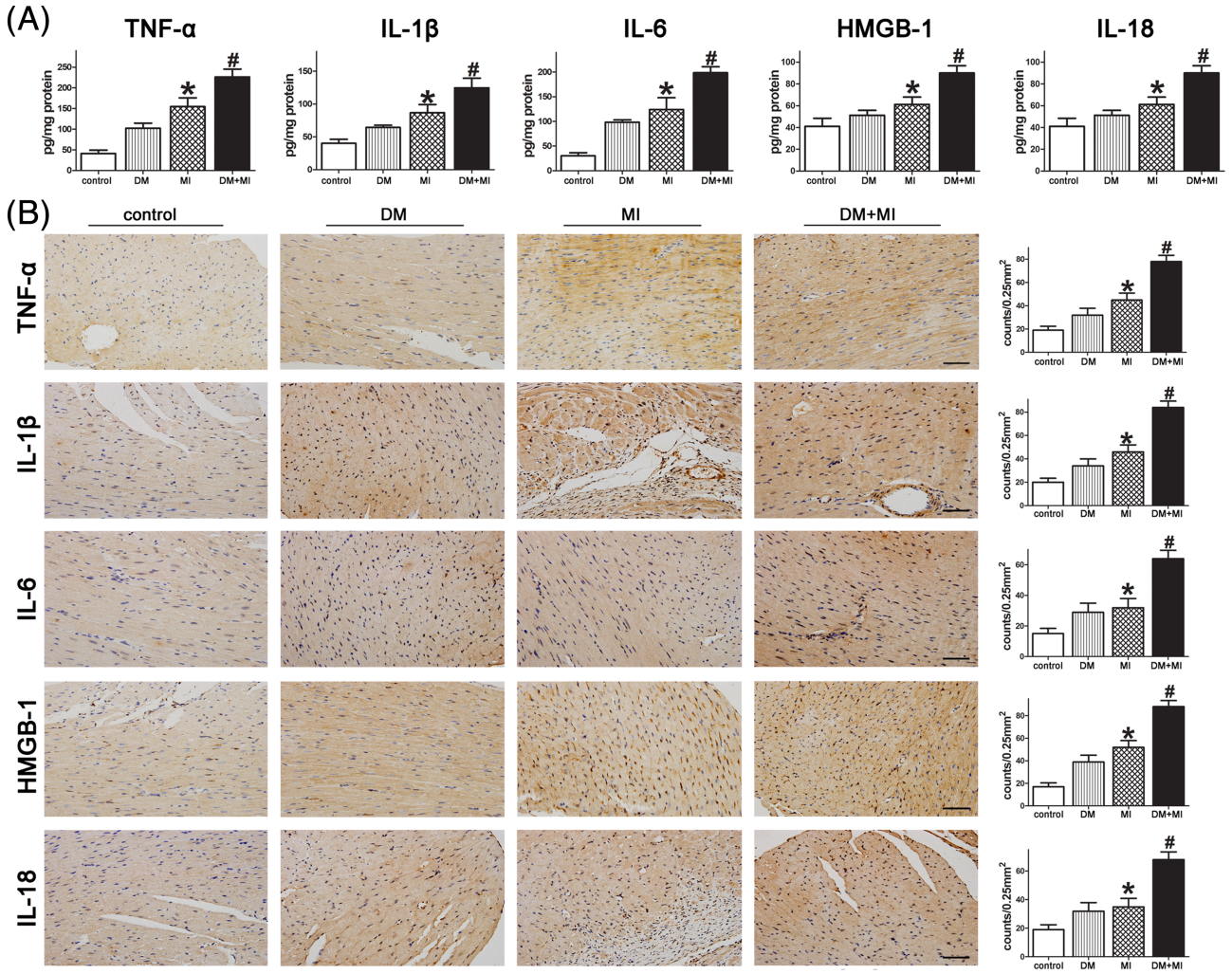

Figure 3 DM increased the expression of inflammatory factors in the myocardium following MI. (A) The myocardial levels of inflammatory factors were analysed by ELISA. (B) Representative immunohistochemical photographs and quantification assay of the myocardium from the MI and DM groups (scale bar = 50 μm). $^{\#}P < 0.05$ DM + MI vs. MI; $^{*}P < 0.05$ MI vs. controls. DM, diabetes mellitus; MI, myocardial infarction.

In parallel, immunoblotting analysis showed a decreased LC3-II/I ratio and increased p62 levels in left ventricular homogenates from DM + MI mice compared with MI mice, indicating impaired autophagy (*Figure 5B*).

To unravel the cell specificity of differential gene expression, we labelled cardiomyocytes from peri-infarct regions using an anti-myoglobin antibody for immunofluorescence staining. Subsequently, the level of LC3 was assessed using a specific LC3 antibody. The results showed decreased accumulation of LC3-positive autophagosomes in peri-infarct regions of the LV in DM mice compared with MI mice, further suggesting that DM causes damaged autophagy in cardiomyocytes in response to MI (*Figure 5C*).

Moreover, electron microscopic images showed an ordered array of myofibres arranged with mitochondria stacked in between them in cardiomyocytes of control mice. Autophagy was activated in the peri-infarct regions of the LV in both the MI and DM + MI groups. Of interest, cardiomyocytes in peri-infarct regions of LV in DM showed increased accumulation of undergraded mitochondria in autophagosomes (*Figure 5D*).

Induction of autophagy attenuated NLRP3 inflammasome and caspase-1 activation in diabetes mellitus mice subjected to myocardial infarction

Considering that accumulating evidence suggests autophagy plays dual roles in cytoprotection and cell death, the effects of autophagy on cardiac remodelling were determined in a DM mouse model of MI. As shown in *Figure 6*,

DOI: 10.1002/ehf2.13754

Figure 4 DM activated the myocardial NLRP3 inflammasome and caspase-1 in mice after MI. (A & B) The mRNA and protein levels of NLRP3 and cleaved caspase-1 were assessed by qPCR and western blotting analysis. Graph right shows densitometric quantification. (C) Representative image of immunofluorescence assays of NLRP3 and cleaved caspase-1 in LV tissue sections from control and DM hearts after MI. DAPI nuclear staining in blue (scale bar = 50 μm). (D) Representative images of TUNEL-positive cells in the myocardium from DM and the control group. Original magnification ×400 (scale bar = 50 mm). $^{\#}P < 0.05$ DM + MI vs. MI; $^{*}P < 0.05$ MI vs. controls. DM, diabetes mellitus; MI, myocardial infarction.

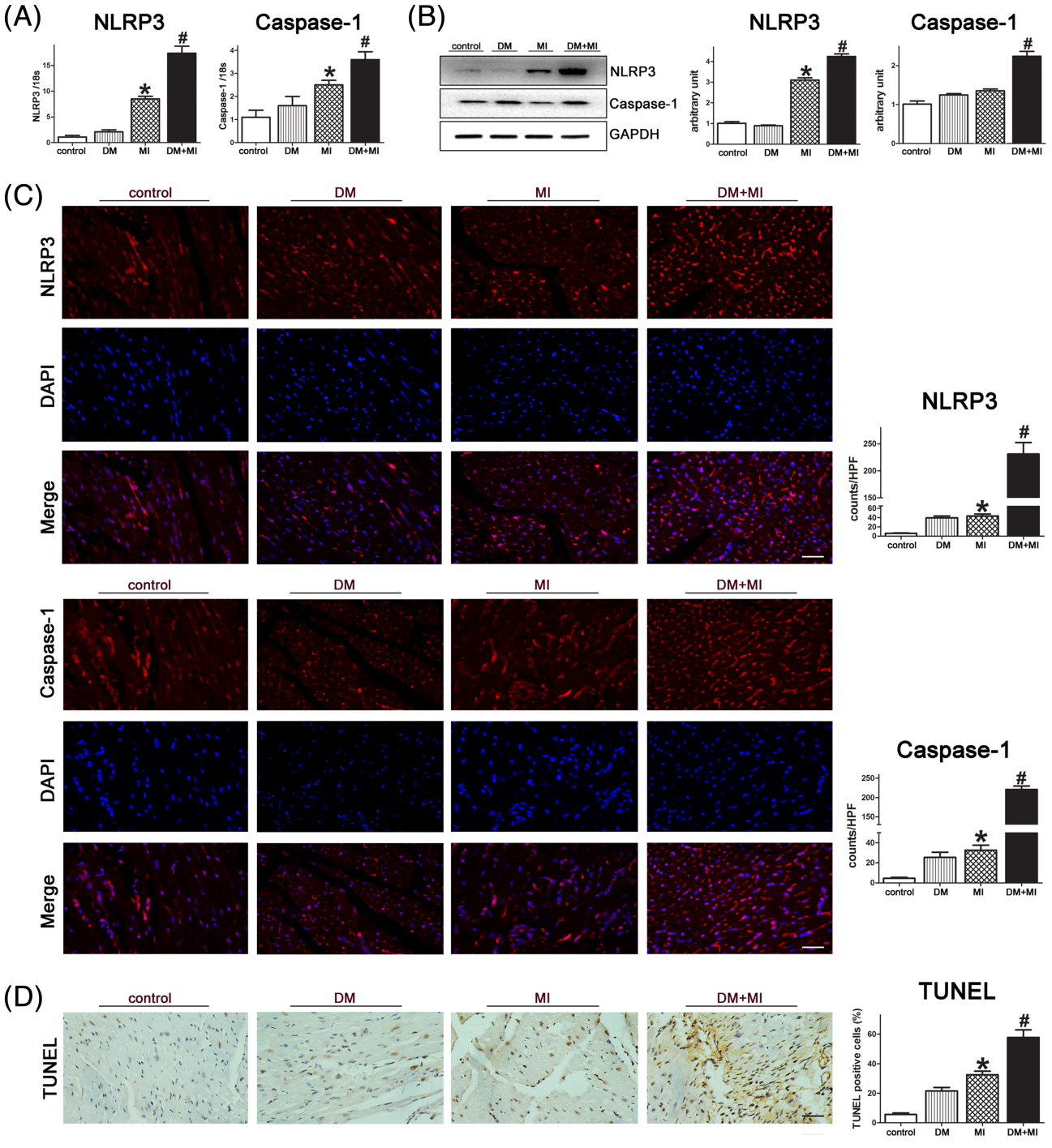

treatment of DM mice subjected to MI with the autophagic inducer rapamycin resulted in a significantly increased LC3-positive autophagosomes in peri-infarct regions of the left ventricle, and attenuated NLRP3 inflammasome and caspase-1 activation. Subsequently, immunofluorescence assays demonstrated that the levels of IL-1β and IL-18 in

Figure 5 DM impaired autophagy in the myocardium of post-infarct mice. (A) Expression levels of genes critical in autophagy in myocardial homogenates from peri-infarct regions of the left ventricle after MI. (B) Western blot analysis of the autophagy proteins LC3 and p62 in myocardial homogenates from peri-infarct regions of the left ventricle after MI. (C) Representative image of immunofluorescence assays of LC3 dots in left ventricle tissue sections of hearts from different groups; red, LC3; blue, DAPI-stained nuclei; green, myoglobin-positive cardiomyocytes (scale bar = 50 μm). (D) Electron micrographs show more autophagic vacuole formation in cardiomyocytes of MI mice in the presence and absence of DM. Quantification of autophagy by measuring the average number of autophagic vacuoles per 100 fields in electron microscope images (scale bars = 500 nm). $^{\#}P < 0.05$ DM + MI vs. MI; $^{*}P < 0.005$ MI vs. controls. DM, diabetes mellitus; MI, myocardial infarction; TEM, transmission electron microscopy.

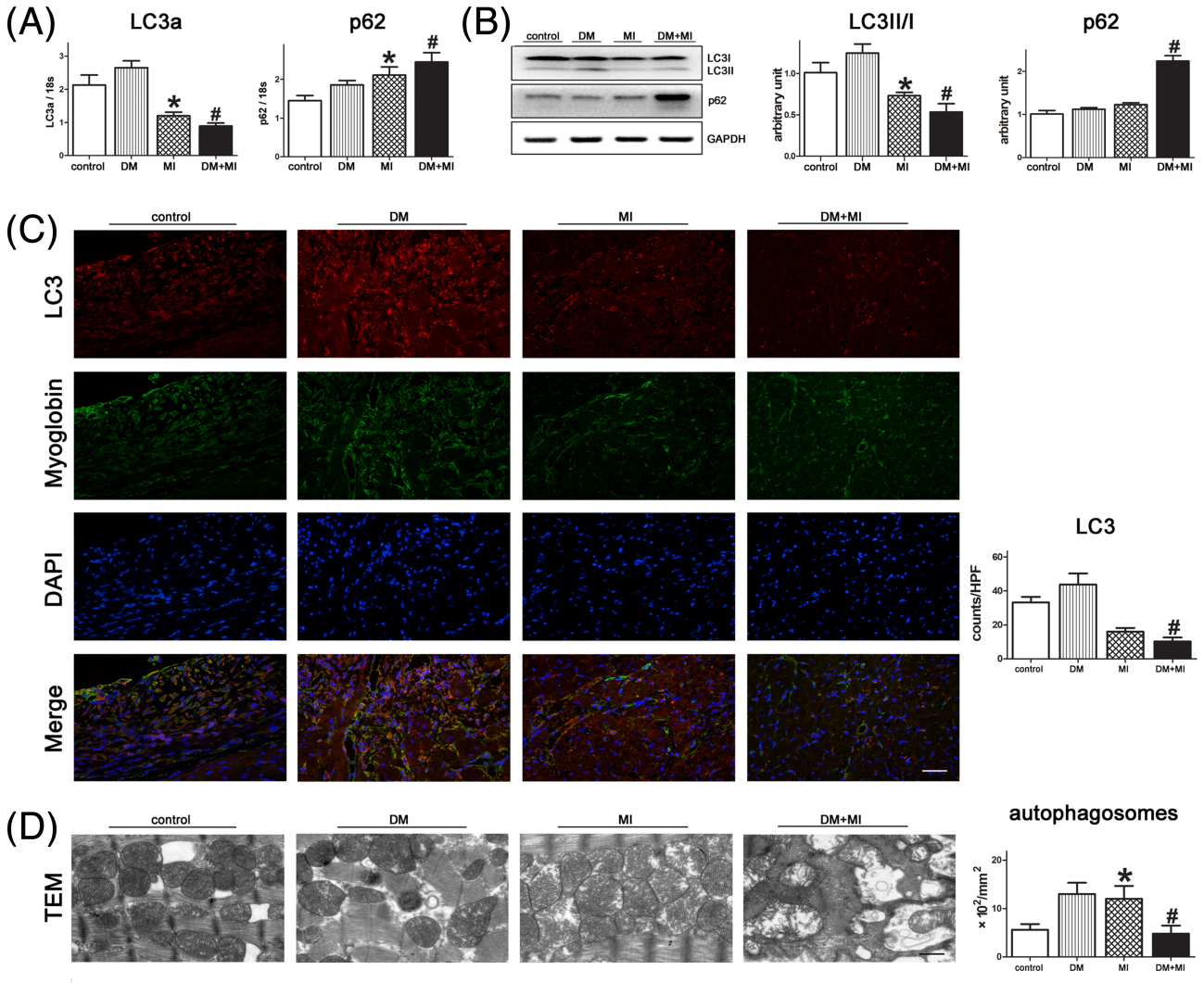

peri-infarct regions of DM + MI mice treated with rapamycin were significantly down-regulated. Furthermore, TUNEL staining also demonstrated that treatment with rapamycin decreased the apoptosis of cardiomyocytes from DM mice subjected to MI.

In contrast, autophagy inhibitors played the opposite role. Treatment of DM + MI mice with the autophagic inhibitor 3MA resulted in significantly increased activation of the NLRP3 inflammasome and caspase-1, a number of TUNEL-positive cells, and mature IL-1β and IL-18 in the peri-infarct regions of the LV (*Figure 6*).

Induction of autophagy attenuated post-infarct cardiac remodelling in diabetes mellitus mice

Moreover, up-regulated autophagy also demonstrated decreased dilatation of LV-internal dimension, LV function, cardiomyocyte size, scar circumference, fibrotic area, the ratio of heart weight to body weight, and increase of LVEF or FS compared with DM mice after MI (*Figure 7*).

In contrast, autophagy inhibition exacerbated the dilatation of the LV chamber dilation, scar expansion, cardiac

DOI: 10.1002/ehf2.13754

Figure 6 Induction of autophagy deteriorates myocardial NLRP3 inflammasome activation in DM mice after MI. Representative pictures and quantification assay of double-immunofluorescence assays of LC3 (scale bar = 50 μm), electron micrographs of autophagosomes (scale bar = 500 nm), immunofluorescence assays of NLRP3 and caspase-1 (scale bar = 50 μm), TUNEL (scale bar = 50 μm), immunohistochemical photographs of IL-1β and IL-18 (scale bar = 50 μm) in peri-infarct regions of left ventricle sections are shown. DM, diabetes mellitus; MI, myocardial infarction.

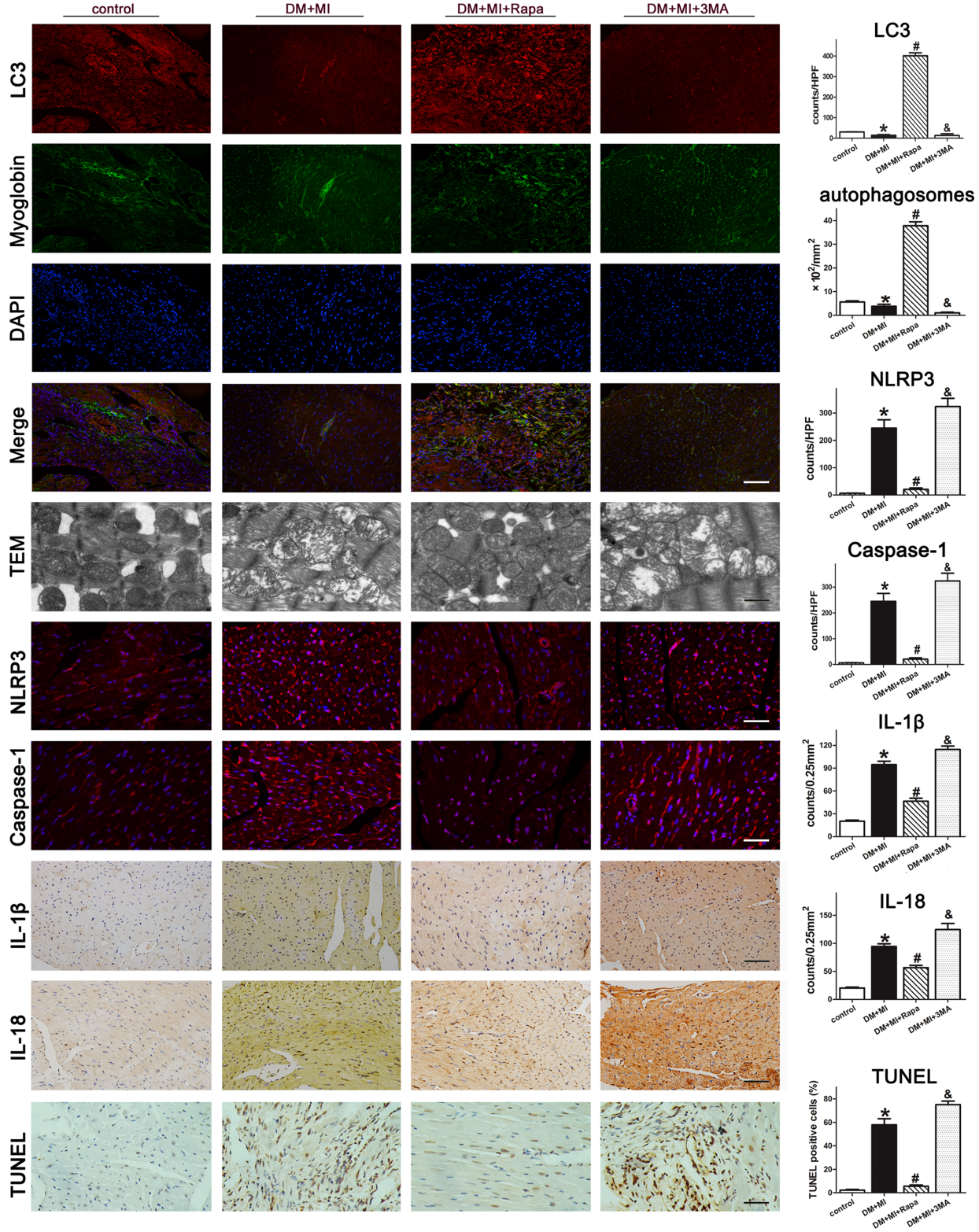

Figure 7 Autophagy inducers mitigated post-infarct cardiac remodelling in DM mice, while NLRP3 inflammasome inhibitors played the opposite role. DM mice suffering from MI were treated with an autophagy inducer or inhibitor, or an NLRP3 inflammasome inhibitor. Representative pictures and quantification assay of echocardiograph M-mode images, haematoxylin and eosin and Masson (scale bar = 50 μm) in left ventricular tissue sections are shown in the upper panels. Quantitative analysis of LVEDV, LVESV, LVEF, LVFS, SV, myocyte size, fibrotic area, and myocardial levels of BNP and cTNT in lower panels. BW, body weight; DM, diabetes mellitus; HW, heart weight; LVEDV, left ventricular end-diastolic volume; LVEF, left ventricular ejection fraction; LVESV, left ventricular end-systolic volume; LVFS, left ventricular fractional shortening; MI, myocardial infarction; SV, systolic volume.

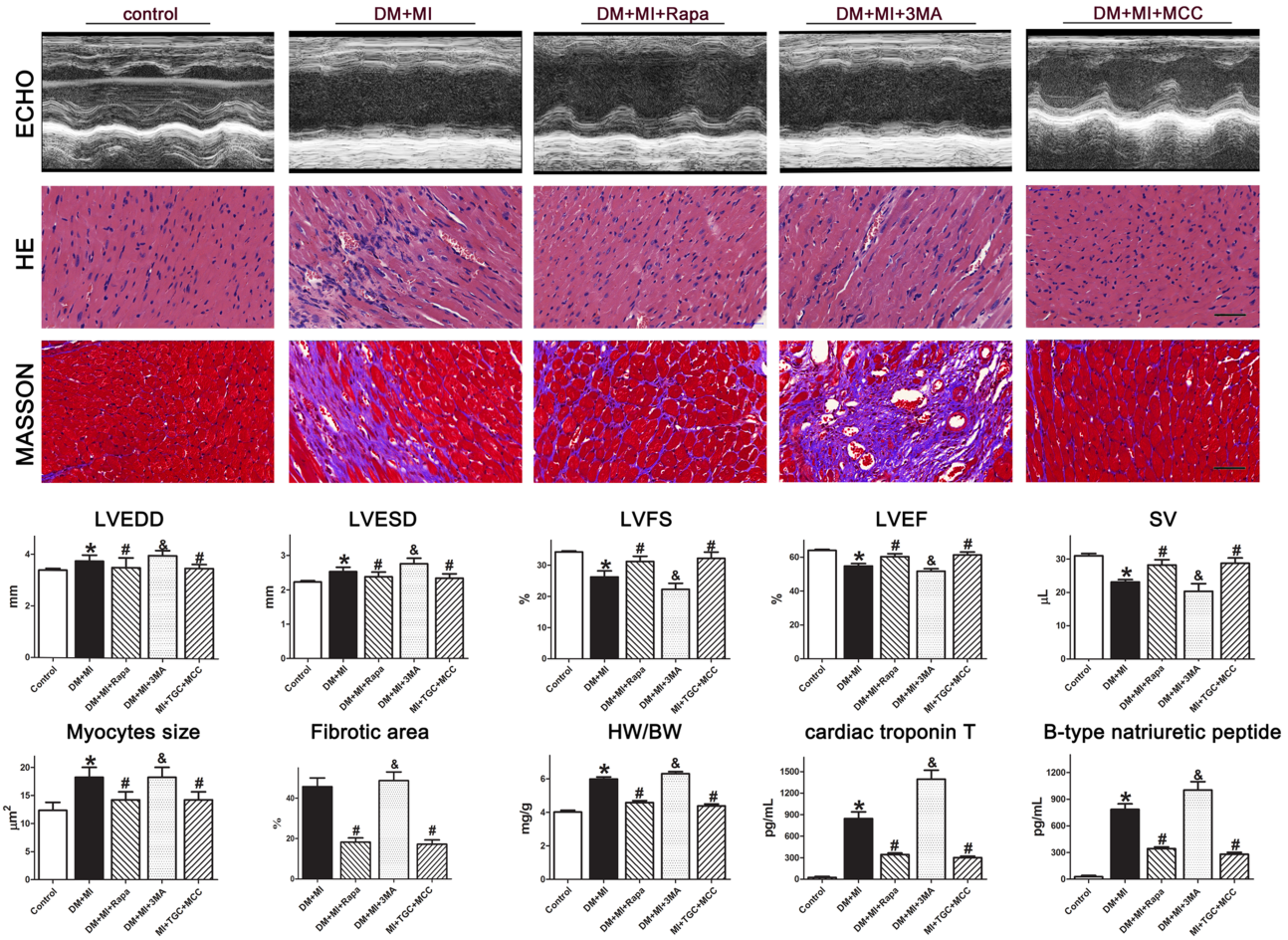

fibrosis, and decreased systolic function compared with DM mice after MI (*Figure 7*).

Taken together, the results indicated that autophagy plays an important protective role against NLRP3 inflammasome activation and cardiac remodelling in DM mice subjected to MI.

Inhibiting NLRP3 inflammasome ameliorated post-infarct cardiac remodelling in diabetes mellitus mice

It was previously reported that NLRP3 inflammasome activation played key role in cardiac remodelling after MI.[25] Thus, we next evaluated whether inhibition of NLRP3 inflammasome ameliorated post-infarct cardiac remodelling in DM mice. As shown in *Figure 7*, treatment DM + MI mice with a specific NLRP3 inflammasome inhibitor, MCC950, indeed ameliorated LV dilation and improved LVEF and FS in post-infarct hearts compared with DM + MI mice. Consequently, the inhibition of NLRP3 inflammasome activity attenuated myocyte size, fibrotic area, the ratio of heart weight to body weight, as well as the levels of myocardial injury biomarkers, cardiac troponin t and B-type peptide (*Figure 7*). Collectively, these results indicated that mitigated NLRP3 inflammasome activation ameliorated post-infarct cardiac remodelling in DM mice.

Discussion

Although considerable improvements in therapies and strategies are currently being made, the presence of DM still

Figure 8 Schematic model depicting mechanisms. Exacerbated post-infarct pathological myocardial remodelling in diabetes is associated with impaired autophagy and aggravated NLRP3 inflammasome activation.

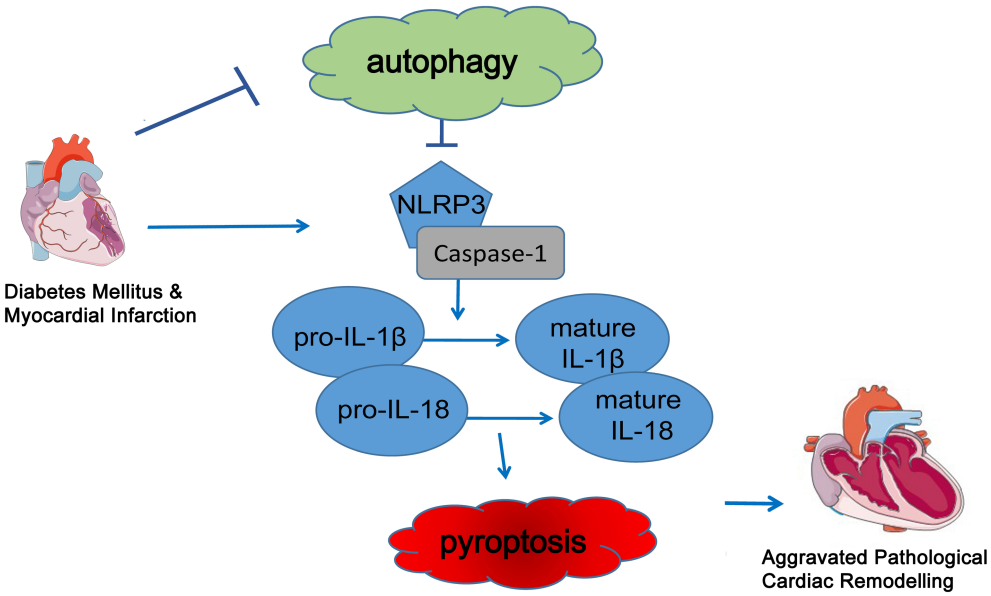

aggravates cardiac dysfunction and doubles the mortality rate of patients with underlying MI. The more complex pathophysiology and a worse prognosis strongly indicate a particular need for a deeper understanding of the interaction of MI in diabetes. Recent data have demonstrated that several mechanisms promote metabolic consequences that impact the dysregulation of microvascular perfusion and energy generation in the cardiomyocytes, subsequently leading to post-infarct cardiac dysfunction in diabetes. One of the important mechanisms deduced mainly from experimental work is the myocardial energy gap between demand and supply. On the one hand, increased oxygen demand in the diabetic myocardium is associated with increased ventricular and vascular stiffness. On the other hand, it decreased the energy supply from myocardial low-perfusion and endothelial dysfunction, and reduced myocellular energy production. This energy mismatch increased inflammasomes in infarct-related segments and impaired autophagy in the remote zones.

In the present study, we provide insights into pathways underlying accelerated pathological myocardial remodelling after MI in a mouse model of T2DM. Integrating molecular characterization, we show an impaired autophagy associated with decreased accumulation of autophagosomes in cardiomyocytes from peri-infarct regions of the LV (*Figure 8*). Furthermore, the NLRP3 inflammasome and caspase-1 were highly activated in cardiomyocytes in the peri-infarct and infarct regions of the LV. This was associated with increased cell pyroptosis and proinflammatory cytokine secretion, thus linking defective autophagy to NLRP3 inflammasome activation.[26,27]

Autophagy involves the removal of damaged cytoplasmic components and organelles to maintain cardiomyocyte function during ischaemic stress.[28] In addition, autophagy prevents activation of pro-death pathways in favour of adaptation to stress.[29] In this paper, a reduced number of autophagosomes but increased amounts of autolysosomes in cardiomyocytes from peri-infarct regions of LV in DM were observed (*Figure 5*). Furthermore, the results at both the transcriptional and posttranscriptional levels demonstrated a decreased LC3 and increased p62 accumulation, further suggesting impaired autophagy. Our observations are in line with a recent study that found cardiac dysfunction in response to MI as a result of inefficient autophagy in DM mice.[30,31]

Accumulating evidence indicates that the NLRP3 inflammasome is a central mediator in the inflammatory response to cardiac ischaemic injury, especially in MI, and activation of the NLRP3 inflammasome amplifies cardiac injury and promotes heart failure.[32] The NLRP3 inflammasome activates caspase-1, triggering inflammatory cell death called pyroptosis by regulating the release of the proinflammatory cytokines IL-1β and IL-18.[33] In the present study, we demonstrated exaggerated NLRP3 inflammasome and caspase-1 activation in DM mice subjected to MI. Importantly, inhibition of the NLRP3 inflammasome attenuated caspase-1 activity and LV pathologic remodelling. These findings are also in line with previous data showing that silencing NLRP3 expression using small interfering RNA or genetic deletion of NLRP3 (knockout) reduced infarct size and limited cardiac dilatation in an experimental MI model in mice.[34,35] Of interest, NLRP3 inflammasome activation was also shown to play an

important role in adverse cardiac remodelling in response to MI under non-diabetic conditions.[36] Thus, inflammasome-dependent caspase-1 activation and subsequent release of IL-18 and IL-1β in cardiomyocytes seem to lead to cardiac remodelling. Accordingly, inhibition of caspase-1 reduced myocardial infarct size, improved cardiac function, and preserved ventricular remodelling.[37] Furthermore, transgenic mice with cardiomyocyte-specific overexpressing caspase-1 show an increased heart failure after MI.[38]

Recent studies have found a mutual relationship between the induction of autophagy and activation of the NLRP3 inflammasome.[39] Autophagy regulates the NLRP3 inflammasome through various mechanisms, including direct inhibition of NLRP3 inflammasome activation and excessive inflammation, by removing sources of endogenous NLRP3 agonists, such as damaged cytoplasmic components and organelles. Earlier reports demonstrated that Atg16L1-deficient macrophages extensively improved IL-1β and IL-18 secretion in the presence of lipopolysaccharide in a Toll/IL-1 receptor domain-containing adaptor inducing IFN-β-dependent manner.[40] Several lines of evidence show that autophagy is also required to control IL-1β secretion by targeting pro-IL-1β for lysosomal degradation.[41] Inhibition of autophagy enhanced IL-1β secretion after stimulation with specific Toll-like receptor ligands, and this effect was demonstrated to depend on the IL-1R signalling pathway.[42] However, further studies are needed to clarify the exact mechanisms by which autophagy plays an essential role in regulating NLRP3 inflammasome activation in DM and MI. This would provide a basis for manipulating the autophagy and inflammasome signalling to control various inflammatory diseases.

Conclusions

Our results suggest that impaired autophagy and exaggerated NLRP3 inflammasome activation may contribute to pathological LV remodelling after MI in DM. Modulation of autophagy together with inhibition of NLRP3 inflammasome activation may offer a novel therapeutic target.

Conflict of interest

All authors declare that they have no conflict of interest.

Funding

This study was funded by National Science Foundation (Grant 81703877, 82074216, &82004135), Science and Technology Planning Project of Guangzhou (202102010301), a Featured Innovative Project from Guangdong Provincial Universities (2019KTSCX029), Young Talents Support Project from China Association of Chinese Medicine (2019-QNRC2-C06), Team of prevention and treatment of acute myocardial infarction with Chinese medicine (2019KCXTD009), and Foundation of Guangdong Province of CM (20211187&20201142). The sponsors have had no role in the project development, in the collection of data, in the preparation of this manuscript, nor the decision to publish.

Supporting information

Additional supporting information may be found online in the Supporting Information section at the end of the article.

Table S1. Treatment schedule.
Table S2. Echocardiographic characteristics. LVEDD, left ventricular end-diastolic diameter; LVESD, left ventricular end-systolic diameter; FS, fractional shortening; and EF, ejection fraction. All values are mean±SE. STZ were administered by intraperitoneal injection; Rapa, rapamycin (autophagy inducer); 3MA (mTOR/autophagy inhibitor); MCC950 (NLRP3 inflammasome inhibitor).

References

1. Gyldenkerne C, Olesen KKW, Madsen M, Thim T, Jensen LO, Raungaard B, Sørensen HT, Bøtker HE, Maeng M. Extent of coronary artery disease is associated with myocardial infarction and mortality in patients with diabetes mellitus. *Clin Epidemiol* 2019; **11**: 419–428.
2. Benjamin EJ, Virani SS, Callaway CW, Chamberlain AM, Chang AR, Cheng S, Chiuve SE, Cushman M, Delling FN, Deo R, de Ferranti SD, Ferguson JF, Fornage M, Gillespie C, Isasi CR, Jiménez MC, Jordan LC, Judd SE, Lackland D, Lichtman JH, Lisabeth L, Liu S, Longenecker CT, Lutsey PL, Mackey JS, Matchar DB, Matsushita K, Mussolino ME, Nasir K, O'Flaherty M, Palaniappan LP, Pandey A, Pandey DK, Reeves MJ, Ritchey MD, Rodriguez CJ, Roth GA, Rosamond WD, Sampson UKA, Satou GM, Shah SH, Spartano NL, Tirschwell DL, Tsao CW, Voeks JH, Willey JZ, Wilkins JT, Wu JH, Alger HM, Wong SS, Muntner P. Heart disease and stroke statistics-2018 update: a report from the American Heart Association. *Circulation* 2018; **137**: e67–e492.
3. Cui J, Liu Y, Li Y, Xu F, Liu Y. Type 2 diabetes and myocardial infarction: recent clinical evidence and perspective. *Front Cardiovasc Med* 2021; **8**: 644189.

4. Pararajasingam G, Løgstrup BB, Høfsten DE, Christophersen TB, Auscher S, Hangaard J, Egstrup K. Dysglycemia and increased left ventricle mass in normotensive patients admitted with a first myocardial infarction: prognostic implications of dysglycemia during 14 years of follow-up. *BMC Cardiovasc Disord* 2019; **19**: 103.
5. Mao S, Vincent M, Chen M, Zhang M, Hinek A. Exploration of multiple signaling pathways through which sodium tanshinone IIA sulfonate attenuates pathologic remodelling experimental infarction. *Front Pharmacol* 2019; **10**: 779.
6. Mao S, Chen P, Li T, Guo L, Zhang M. Tongguan capsule mitigates post-myocardial infarction remodelling by promoting autophagy and inhibiting apoptosis: role of Sirt1. *Front Physiol* 2018; **9**: 589.
7. Byrne NJ, Matsumura N, Maayah ZH, Ferdaoussi M, Takahara S, Darwesh AM, Levasseur JL, Jahng JWS, Vos D, Parajuli N, El-Kadi AOS, Braam B, Young ME, Verma S, Light PE, Sweeney G, Seubert JM, Dyck JRB. Empagliflozin blunts worsening cardiac dysfunction associated with reduced NLRP3 (nucleotide-binding domain-like receptor protein 3) inflammasome activation in heart failure. *Circ Heart Fail* 2020; **13**: e006277.
8. Kaneko N, Kurata M, Yamamoto T, Morikawa S, Masumoto J. The role of interleukin-1 in general pathology. *Inflamm Regen* 2019; **39**: 12.
9. Nicolás-Ávila JA, Lechuga-Vieco AV, Esteban-Martínez L, Sánchez-Díaz M, Díaz-García E, Santiago DJ, Rubio-Ponce A, Li JL, Balachander A, Quintana JA, Martínez-de-Mena R, Castejón-Vega B, Pun-García A, Través PG, Bonzón-Kulichenko E, García-Marqués F, Cussó L, A-González N, González-Guerra A, Roche-Molina M, Martin-Salamanca S, Crainiciuc G, Guzmán G, Larrazabal J, Herrero-Galán E, Alegre-Cebollada J, Lemke G, Rothlin CV, Jimenez-Borreguero LJ, Reyes G, Castrillo A, Desco M, Muñoz-Cánoves P, Ibáñez B, Torres M, Ng LG, Priori SG, Bueno H, Vázquez J, Cordero MD, Bernal JA, Enríquez JA, Hidalgo A. A network of macrophages supports mitochondrial homeostasis in the heart. *Cell* 2020; **183**: 94–109.e23.
10. Ljubojević-Holzer S, Kraler S, Djalinac N, Abdellatif M, Voglhuber J, Schipke J, Schmidt M, Kling KM, Franke GT, Herbst V, Zirlik A, von Lewinski D, Scherr D, Rainer PP, Kohlhaas M, Nickel A, Mühlfeld C, Maack C, Sedej S. Loss of autophagy protein ATG5 impairs cardiac capacity in mice and humans through diminishing mitochondrial abundance and disrupting Ca2+ cycling. *Cardiovasc Res* 2021.
11. Völkers M, Doroudgar S, Nguyen N, Konstandin MH, Quijada P, Din S, Ornelas L, Thuerauf DJ, Gude N, Friedrich K, Herzig S, Glembotski CC, Sussman MA. PRAS40 prevents development of diabetic cardiomyopathy and improves hepatic insulin sensitivity in obesity. *EMBO Mol Med* 2014; **6**: 57–65.
12. Das A, Durrant D, Koka S, Salloum FN, Xi L, Kukreja RC. Mammalian target of rapamycin (mTOR) inhibition with rapamycin improves cardiac function in type 2 diabetic mice: potential role of attenuated oxidative stress and altered contractile protein expression. *J Biol Chem* 2014; **289**: 4145–4160.
13. Li MH, Zhang YJ, Yu YH, Yang SH, Iqbal J, Mi QY, Li B, Wang ZM, Mao WX, Xie HG, Chen SL. Berberine improves pressure overload-induced cardiac hypertrophy and dysfunction through enhanced autophagy. *Eur J Pharmacol* 2014; **728**: 67–76.
14. Fidler TP, Marti A, Gerth K, Middleton EA, Campbell RA, Rondina MT, Weyrich AS, Abel ED. Glucose metabolism is required for platelet hyperactivation in a murine model of type 1 diabetes. *Diabetes* 2019; **68**: 932–938.
15. Poucher SM, Cheetham S, Francis J, Zinker B, Kirby M, Vickers SP. Effects of saxagliptin and sitagliptin on glycaemic control and pancreatic β-cell mass in a streptozotocin-induced mouse model of type 2 diabetes. *Diabetes Obes Metab* 2012; **14**: 918–926.
16. Yurre AR, Martins EGL, Lopez-Alarcon M, Cabral B, Vera N, Lopes JA, Galina A, Takiya CM, Lindoso RS, Vieyra A, SÁenz OC, Medei E. Type 2 diabetes mellitus alters cardiac mitochondrial content and function in a non-obese mice model. *An Acad Bras Cienc* 2020; **92**: e20191340.
17. Sendler M, van den Brandt C, Glaubitz J, Wilden A, Golchert J, Weiss FU, Homuth G, De Freitas Chama LL, Mishra N, Mahajan UM, Bossaller L, Völker U, Bröker BM, Mayerle J, Lerch MM. NLRP3 inflammasome regulates development of systemic inflammatory response and compensatory anti-inflammatory response syndromes in mice with acute pancreatitis. *Gastroenterology* 2020; **158**: 253–269.e14.
18. Jiang T, Zhan F, Rao Z, Pan X, Zhong W, Sun Y, Wang P, Lu L, Zhou H, Wang X. Combined ischemic and rapamycin preconditioning alleviated liver ischemia and reperfusion injury by restoring autophagy in aged mice. *Int Immunopharmacol* 2019; **74**: 105711.
19. Mao S, Ma H, Chen P, Liang Y, Zhang M, Hinek A. Fat-1 transgenic mice rich in endogenous omega-3 fatty acids are protected from lipopolysaccharide-induced cardiac dysfunction. *ESC Heart Fail* 2021; **8**: 1966–1978.
20. Mao S, Li W, Qa'aty N, Vincent M, Zhang M, Hinek A. Tanshinone IIA inhibits angiotensin II induced extracellular matrix remodeling in human cardiac fibroblasts—implications for treatment of pathologic cardiac remodeling. *Int J Cardiol* 2016; **202**: 110–117.
21. Sokolova M, Sjaastad I, Louwe MC, Alfsnes K, Aronsen JM, Zhang L, Haugstad SB, Bendiksen BA, Øgaard J, Bliksøen M, Lien E, Berge RK, Aukrust P, Ranheim T, Yndestad A. NLRP3 inflammasome promotes myocardial remodelling during diet-induced obesity. *Front Immunol* 2019; **10**: 1621.
22. Mishra PK, Adameova A, Hill JA, Baines CP, Kang PM, Downey JM, Narula J, Takahashi M, Abbate A, Piristine HC, Kar S, Su S, Higa JK, Kawasaki NK, Matsui T. Guidelines for evaluating myocardial cell death. *Am J Physiol Heart Circ Physiol* 2019; **317**: H891–h922.
23. Singla DK, Johnson TA, Tavakoli Dargani Z. Exosome treatment enhances anti-inflammatory M2 macrophages and reduces inflammation-induced pyroptosis in doxorubicin-induced cardiomyopathy. *Cell* 2019; **8**: 1224.
24. Tan VP, Smith JM, Tu M, Yu JD, Ding EY, Miyamoto S. Dissociation of mitochondrial HK-II elicits mitophagy and confers cardioprotection against ischemia. *Cell Death Dis* 2019; **10**: 730.
25. Butts B, Gary RA, Dunbar SB, Butler J. The importance of NLRP3 inflammasome in heart failure. *J Card Fail* 2015; **21**: 586–593.
26. Biasizzo M, Kopitar-Jerala N. Interplay between NLRP3 inflammasome and autophagy. *Front Immunol* 2020; **11**: 591803.
27. Nagoor Meeran MF, Azimullah S, Laham F, Tariq S, Goyal SN, Adeghate E, Ojha S. α-Bisabolol protects against β-adrenergic agonist-induced myocardial infarction in rats by attenuating inflammation, lysosomal dysfunction, NLRP3 inflammasome activation and modulating autophagic flux. *Food Funct* 2020; **11**: 965–976.
28. Chang JC, Hu WF, Lee WS, Lin JH, Ting PC, Chang HR, Shieh KR, Chen TI, Yang KT. Intermittent hypoxia induces autophagy to protect cardiomyocytes from endoplasmic reticulum stress and apoptosis. *Front Physiol* 2019; **10**: 995.
29. Ma S, Wang Y, Chen Y, Cao F. The role of the autophagy in myocardial ischemia/reperfusion injury. *Biochim Biophys Acta* 2015; **1852**: 271–276.
30. Durga Devi T, Babu M, Mäkinen P, Kaikkonen MU, Heinaniemi M, Laakso H, Ylä-Herttuala E, Rieppo L, Liimatainen T, Naumenko N, Tavi P, Ylä-Herttuala S. Aggravated postinfarct heart failure in type 2 diabetes is associated with impaired mitophagy and exaggerated inflammasome activation. *Am J Pathol* 2017; **187**: 2659–2673.
31. Kanamori H, Naruse G, Yoshida A, Minatoguchi S, Watanabe T, Kawaguchi T, Yamada Y, Mikami A, Kawasaki M, Takemura G, Minatoguchi S. Metformin enhances autophagy and provides cardioprotection in δ-sarcoglycan deficiency-induced dilated cardiomyopathy. *Circ Heart Fail* 2019; **12**: e005418.
32. Toldo S, Abbate A. The NLRP3 inflammasome in acute myocardial infarction. *Nat Rev Cardiol* 2018; **15**: 203–214.

33. Mauro AG, Bonaventura A, Mezzaroma E, Quader M, Toldo S. NLRP3 inflammasome in acute myocardial infarction. *J Cardiovasc Pharmacol* 2019; **74**: 175–187.
34. Mezzaroma E, Toldo S, Farkas D, Seropian IM, Van Tassell BW, Salloum FN, Kannan HR, Menna AC, Voelkel NF, Abbate A. The inflammasome promotes adverse cardiac remodelling following acute myocardial infarction in the mouse. *Proc Natl Acad Sci U S A* 2011; **108**: 19725–19730.
35. Mezzaroma E, Toldo S, Abbate A. Role of NLRP3 (cryopyrin) in acute myocardial infarction. *Cardiovasc Res* 2013; **99**: 225–226.
36. Li X, Yang W, Ma W, Zhou X, Quan Z, Li G, Liu D, Zhang Q, Han D, Gao B, Li C, Wang J, Kang F. (18)F-FDG PET imaging-monitored anti-inflammatory therapy for acute myocardial infarction: exploring the role of MCC950 in murine model. *J Nucl Cardiol* 2020; **28**: 2346–2357.
37. Audia JP, Yang XM, Crockett ES, Housley N, Haq EU, O'Donnell K, Cohen MV, Downey JM, Alvarez DF. Caspase-1 inhibition by VX-765 administered at reperfusion in P2Y(12) receptor antagonist-treated rats provides long-term reduction in myocardial infarct size and preservation of ventricular function. *Basic Res Cardiol* 2018; **113**: 32.
38. Merkle S, Frantz S, Schön MP, Bauersachs J, Buitrago M, Frost RJ, Schmitteckert EM, Lohse MJ, Engelhardt S. A role for caspase-1 in heart failure. *Circ Res* 2007; **100**: 645–653.
39. Harris J, Lang T, Thomas JPW, Sukkar MB, Nabar NR, Kehrl JH. Autophagy and inflammasomes. *Mol Immunol* 2017; **86**: 10–15.
40. Saitoh T, Fujita N, Jang MH, Uematsu S, Yang BG, Satoh T, Omori H, Noda T, Yamamoto N, Komatsu M, Tanaka K, Kawai T, Tsujimura T, Takeuchi O, Yoshimori T, Akira S. Loss of the autophagy protein Atg16L1 enhances endotoxin-induced IL-1beta production. *Nature* 2008; **456**: 264–268.
41. de Lavera I, Pavon AD, Paz MV, Oropesa-Avila M, de la Mata M, Alcocer-Gomez E, Garrido-Maraver J, Cotan D, Alvarez-Cordoba M, Sanchez-Alcazar JA. The connections among autophagy, inflammasome and mitochondria. *Curr Drug Targets* 2017; **18**: 1030–1038.
42. de Castro CP, Jones SA, Cheallaigh CN, Hearnden CA, Williams L, Winter J, Lavelle EC, Mills KH, Harris J. Autophagy regulates IL-23 secretion and innate T cell responses through effects on IL-1 secretion. *J Immunol* 2012; **189**: 4144–4153.